Journal of Organometallic Chemistry, 329 (1987) 405–412
Elsevier Sequoia S.A., Lausanne – Printed in The Netherlands

Synthesis and structural characterisation of $[Pt_3Au(\mu_2\text{-}CO)_3(PPh_3)_5]NO_3$

J.J. Bour*, R.P.F. Kanters, P.P.J. Schlebos, W. Bos, W.P. Bosman, H. Behm, Paul T. Beurskens and J.J. Steggerda

Inorganic Chemistry and Crystallography, Faculty of Science, Toernooiveld, 6525 ED Nijmegen (The Netherlands)

(Received February 5th, 1987)

Abstract

The compound $[Pt_3Au(\mu_2\text{-}CO)_3(PPh_3)_5]NO_3$ was formed as the main product of the reaction of $AuPPh_3NO_3$ with $Pt(PPh_3)_3$ and CO. Its structure was determined by X-ray diffraction, using Cu-K_α radiation with a graphite crystal monochromator; λ 1.54184 Å, $AuC_{93}H_{75}NO_6P_5Pt_3 \cdot 1/2\ C_4H_{10}O$, $M_r = 2276.80$, triclinic, space group $P\bar{1}$, a 15.256(2), b 14.422(2), c 21.663(3) Å, α 93.138(9), β 91.823(9), γ 68.654(9)°, V 4432(3) Å^3, $Z = 2$, D_c 1.678 Mg/m^3, μ(Cu-K_α) 131.8 cm^{-1}, $F(000) = 2194$, T 290 K. Final conventional R factor = 0.063, $R_w = 0.078$ for 11193 unique reflections and 322 variables. The structure was solved by automated Patterson methods. The metal cluster is a strongly distorted tetrahedron with one short (2.700(1) Å) and two longer (2.906(1) Å) Pt–Au distances. This bonding asymmetry is discussed in a comparison with known structures of similar 54 and 56 valence electron Pt_3Au clusters.

Introduction

Heterometallic cluster compounds have attracted wide attention in recent years and many clusters containing gold are known. Several types of platinum–gold cluster compounds have been reported [1–5]. In the course of our investigations of the reaction of CO and H_2 with $AuPPh_3NO_3$, which lead to gold clusters and fulminato compounds [6], we also studied the reaction of $AuPPh_3NO_3$ with $Pt(PPh_3)_3$ and CO. We report here on $[Pt_3Au(\mu_2\text{-}CO)_3]_5]NO_3$, which was the main reaction product. The structure of the 56 electron cluster $[Pt_3Au(\mu_2\text{-}CO)_3(PPh_3)_5]^+$ (I) was determined, and is compared with that of the 54 electron cluster $[Pt_3Au(\mu_2\text{-}CO)_3(Pcy_3)_4]^+$ (II).

Experimental

$AuPPh_3NO_3$ and $Pt(PPh_3)_3$ were prepared by established procedures [7,8]. Preparation of $AuPt_3(CO)_3(PPh_3)_5NO_3$. To a solution of 200 mg $Pt(PPh_3)_3$ in 10 ml of acetone was added 203 mg of $AuPPh_3NO_3$ (molar ratio 1/2), and CO was bubbled through the solution for 10 min. Within a few minutes the colour changed from orange to dark red, and after 6 h became orange again. After 24 h the crystalline precipitate was filtered off and recrystallised from methylene chloride/ether. The product was washed with acetone and ether and dried in vacuo. Yield 100 mg. Anal. Found: Au, 9.25; Pt, 27.40; C, 50.10; H, 3.55; N, 0.62. $AuPt_3P_5C_{93}H_{75}NO_6$ calc: Au, 8.79; Pt, 26.13; C, 49.87; H, 3.38; N, 0.63%; M = 2239.69. Infrared (CsI pellet) $\nu(NO_3^-)$, 1360 cm^{-1}; $\nu(CO)$, 1830, 1850 cm^{-1}.

Crystal structure determination

A crystal mounted in a capillary containing a drop of diethyl ether (to slow down the deterioration of the crystal) was used for the X-ray analysis. Cu-K_α radiation was used with a graphite crystal monochromator on a Nonius CAD4 single crystal diffractometer (λ 1.54184 Å). The unit cell dimensions were determined from the angular settings of 25 reflections with $26° < \theta < 40°$. Space group $P\bar{1}$ was confirmed by the structure determination. The intensity data of 16432 reflections (up to $\theta = 40°$) were measured, using the $\theta - 2\theta$ scan technique, with a scan angle of 1.50° and a variable scan rate with a maximum scan time of 20 s per reflection. The intensity of the primary beam was checked throughout the data collection by monitoring three reference reflections every 30 min. Decomposition of the crystal was apparent. The drift correction factors for these three reflections increases monotonically from 1.00 to 1.36, 2.16 and 1.81 respectively (average: 1.83). The differences between these correction curves are ascribed to the anisotropic effect of decomposition. A smooth curve based on the average correction factors was used to correct for this decomposition. A profile analysis was performed on all the reflections [9,10]; empirical absorption correction was applied, using psi-scans [11] (Correction factors were in the range 0.87 to 1.00). Space group symmetry equivalent reflections were averaged, $R_{int} = \Sigma\ (I - \langle I \rangle)/\Sigma I = 0.02$, resulting in 13117 unique reflections, of which 11193 were observed with $I > 3\sigma(I)$. No extinction correction, Lorentz and polarization corrections were applied, and the data were reduced to $|F_o|$ values.

The structure was solved fully automatically by PATSYS [12] which combines the Patterson parts of SHELX84 [13] and DIRDIF [14]. All the nonhydrogen atoms were located in one run. Most hydrogen atoms were located from difference Fourier maps and were included in the refinement. The phenyl rings were treated as regular hexagons and their hydrogen atoms placed at ideal positions. A difference Fourier map showed the presence of electron density around a crystallographic center of symmetry, and this was attributed to partial occupation by a diethyl ether molecule. The occupation factors of oxygen and carbon atoms of the diethyl ether molecule were in the range 0.35–0.58 and so we assumed the presence of one disordered

(*Continued on p. 409*)

Table 1

Selected fractional positional and thermal parameters (with esd's)

Atom	x	y	z	U_{eq} ($\times 100$)
Au(1)	0.08274(4)	0.19450(4)	0.27619(2)	2.34(1)
Pt(2)	0.18870(4)	0.15060(4)	0.17351(2)	1.56(1)
Pt(3)	0.24796(4)	0.01402(4)	0.26110(2)	2.09(1)
Pt(4)	0.27654(4)	0.18536(4)	0.27789(2)	2.04(1)
P(1)	−0.0210(3)	0.2410(3)	0.3560(2)	3.14(14)
P(21)	0.0481(2)	0.2313(3)	0.1198(1)	2.14(12)
P(22)	0.3179(2)	0.0908(3)	0.1024(2)	2.19(12)
P(3)	0.2843(3)	−0.1412(3)	0.2937(2)	2.89(14)
P(4)	0.3362(3)	0.2868(3)	0.3331(2)	3.13(15)
O(1)	0.2145(7)	0.3550(7)	0.1896(4)	4.3(3)
O(2)	0.1674(7)	−0.0553(7)	0.1463(4)	4.0(3)
O(3)	0.3632(8)	0.0333(8)	0.3759(5)	5.8(3)
C(1)	0.2251(8)	0.2768(8)	0.2064(5)	1.2(3)
C(2)	0.1868(9)	0.0032(10)	0.1777(6)	2.7(3)
C(3)	0.3191(10)	0.0647(11)	0.3311(6)	3.6(4)
N(1)	0.1948(20)	0.1930(23)	0.7315(15)	14.2(9)
O(11)	0.1718(16)	0.1524(19)	0.7751(12)	18.6(9)
O(12)	0.2396(23)	0.1449(24)	0.6910(15)	23.6(14)
O(13)	0.2113(21)	0.2577(24)	0.7591(14)	22.9(13)
C(111)	0.1229(6)	0.2059(8)	0.4422(4)	4.3(4)
C(112)	0.1637(6)	0.1866(8)	0.5010(4)	5.8(5)
C(113)	0.1141(6)	0.1672(8)	0.5484(4)	5.0(4)
C(114)	0.0236(6)	0.1671(8)	0.5372(4)	5.3(5)
C(115)	−0.0173(6)	0.1864(8)	0.4784(4)	4.4(4)
C(116)	0.0325(6)	0.2057(8)	0.4310(4)	3.2(3)
C(121)	−0.1318(8)	0.4279(8)	0.3128(4)	5.4(5)
C(122)	−0.1777(8)	0.5311(8)	0.3178(4)	7.7(6)
C(123)	−0.1818(8)	0.5821(8)	0.3749(4)	8.3(6)
C(124)	−0.1400(8)	0.5299(8)	0.4270(4)	8.3(6)
C(125)	−0.0940(8)	0.4266(8)	0.4220(4)	5.6(5)
C(126)	−0.0899(8)	0.3757(8)	0.3649(4)	4.4(4)
C(131)	−0.0778(6)	0.0817(8)	0.3449(5)	5.4(5)
C(132)	−0.1422(6)	0.0337(8)	0.3362(5)	7.1(5)
C(133)	−0.2380(6)	0.0896(8)	0.3300(5)	7.1(6)
C(134)	−0.2695(6)	0.1934(8)	0.3326(5)	6.7(5)
C(135)	−0.2052(6)	0.2414(8)	0.3414(5)	5.7(5)
C(136)	−0.1094(6)	0.1856(8)	0.3475(5)	4.0(4)
C(211)	0.0990(6)	0.2208(8)	−0.0044(4)	3.0(3)
C(212)	0.1006(2)	0.1884(6)	−0.0663(4)	3.9(4)
C(213)	0.0465(6)	0.1324(6)	−0.0865(4)	5.0(4)
C(214)	−0.0090(6)	0.1088(6)	−0.0447(4)	5.8(5)
C(215)	−0.0105(6)	0.1413(6)	0.0173(4)	3.7(4)
C(216)	0.0435(6)	0.1973(6)	0.0374(4)	2.4(3)
C(221)	0.0025(6)	0.4155(7)	0.1819(3)	3.6(4)
C(222)	−0.0399(6)	0.5188(7)	0.1891(3)	5.0(4)
C(223)	−0.0757(6)	0.5756(7)	0.1377(3)	6.2(5)
C(224)	−0.0690(6)	0.5288(7)	0.0790(3)	6.4(5)
C(225)	−0.0266(6)	0.4254(7)	0.0718(3)	4.3(4)
C(226)	0.0092(6)	0.3687(7)	0.1232(3)	2.8(3)
C(231)	−0.0533(5)	0.1252(6)	0.1690(4)	3.3(3)
C(232)	−0.1348(5)	0.1105(6)	0.1852(4)	4.9(4)
C(233)	−0.2223(5)	0.1868(6)	0.1792(4)	5.5(5)

continued

Table 1 (continued)

Atom	x	y	z	U_{eq} (× 100)
C(234)	−0.2282(5)	0.2779(6)	0.1570(4)	5.8(5)
C(235)	−0.1467(5)	0.2927(6)	0.1408(4)	4.6(4)
C(236)	−0.0592(5)	0.2163(6)	0.1468(4)	2.6(3)
C(241)	0.4598(6)	0.0055(7)	0.1902(4)	3.6(4)
C(242)	0.5503(6)	−0.0204(7)	0.2156(4)	4.6(4)
C(243)	0.6168(6)	0.0091(7)	0.1882(4)	5.0(4)
C(244)	0.5930(6)	0.0645(7)	0.1353(4)	5.6(5)
C(245)	0.5025(6)	0.0904(7)	0.1098(4)	3.5(4)
C(246)	0.4360(6)	0.0610(7)	0.1373(4)	2.5(3)
C(251)	0.3026(7)	0.2719(7)	0.0554(3)	4.5(4)
C(252)	0.2999(7)	0.3363(7)	0.0090(3)	5.6(5)
C(253)	0.3142(7)	0.3003(7)	−0.0524(3)	5.3(5)
C(254)	0.3312(7)	0.2000(7)	−0.0674(3)	4.4(4)
C(255)	0.3340(7)	0.1356(7)	−0.0210(3)	3.5(4)
C(256)	0.3197(7)	0.1716(7)	0.0404(3)	2.8(3)
C(261)	0.4129(5)	−0.1094(7)	0.0598(4)	4.0(4)
C(262)	0.4193(5)	−0.1957(7)	0.0248(4)	4.8(4)
C(263)	0.3419(5)	−0.1993(7)	−0.0099(4)	6.1(5)
C(264)	0.2581(5)	−0.1166(7)	−0.0096(4)	4.4(4)
C(265)	0.2516(5)	−0.0303(7)	0.0254(4)	3.3(3)
C(266)	0.3291(5)	−0.0267(7)	0.0601(4)	2.5(3)
C(311)	0.2413(8)	−0.3124(9)	0.2626(6)	9.3(7)
C(312)	0.1783(8)	−0.3617(9)	0.2526(6)	10.7(8)
C(313)	0.0821(8)	−0.3071(9)	0.2471(6)	12.7(10)
C(314)	0.0490(8)	−0.2032(9)	0.2515(6)	9.5(7)
C(315)	0.1120(8)	−0.1539(9)	0.2614(6)	6.1(5)
C(316)	0.2082(8)	−0.2085(9)	0.2670(6)	5.0(4)
C(321)	0.4141(8)	−0.2581(9)	0.2084(5)	7.7(6)
C(322)	0.5047(8)	−0.3053(9)	0.1853(5)	9.3(7)
C(323)	0.5826(8)	−0.3094(9)	0.2222(5)	9.1(7)
C(324)	0.5699(8)	−0.2661(9)	0.2820(5)	9.3(7)
C(325)	0.4793(8)	−0.2189(9)	0.3051(5)	7.8(6)
C(326)	0.4014(8)	−0.2149(9)	0.2683(5)	3.5(4)
C(331)	0.3314(7)	−0.2439(7)	0.4028(5)	5.8(5)
C(332)	0.3199(7)	−0.2535(7)	0.4655(5)	8.6(7)
C(333)	0.2579(7)	−0.1739(7)	0.5004(5)	6.9(5)
C(334)	0.2074(7)	−0.0846(7)	0.4727(5)	7.0(5)
C(335)	0.2189(7)	−0.0749(7)	0.4100(5)	4.9(4)
C(336)	0.2809(7)	−0.1546(7)	0.3751(5)	3.0(3)
C(411)	0.4433(8)	0.2867(7)	0.2311(5)	5.7(5)
C(412)	0.4953(8)	0.3230(7)	0.1938(5)	8.5(6)
C(413)	0.5172(8)	0.4055(7)	0.2143(5)	6.6(5)
C(414)	0.4870(8)	0.4517(7)	0.2721(5)	11.4(8)
C(415)	0.4350(8)	0.4154(7)	0.3094(5)	10.2(8)
C(416)	0.4131(8)	0.3329(7)	0.2889(5)	3.5(4)
C(421)	0.5005(8)	0.1647(9)	0.3856(4)	6.3(5)
C(422)	0.5562(8)	0.1085(9)	0.4325(4)	10.0(8)
C(423)	0.5214(8)	0.1195(9)	0.4923(4)	7.7(6)
C(424)	0.4308(8)	0.1867(9)	0.5051(4)	8.9(7)
C(425)	0.3751(8)	0.2429(9)	0.4582(4)	6.2(5)
C(426)	0.4100(8)	0.2319(9)	0.3984(4)	3.9(4)
C(431)	0.1532(7)	0.4210(7)	0.3419(4)	4.3(4)
C(432)	0.0809(7)	0.5098(7)	0.3609(4)	6.2(5)
C(433)	0.0998(7)	0.5762(7)	0.4030(4)	7.6(6)
C(434)	0.1909(7)	0.5556(7)	0.4261(4)	7.6(6)
C(435)	0.2633(7)	0.4677(7)	0.4072(4)	6.0(5)
C(436)	0.2444(7)	0.4004(7)	0.3651(4)	3.6(4)

Table 1 (continued)

Atom	x	y	z	U_{eq} ($\times 100$)
C(51) [a]	0.589(4)	0.515(3)	0.413(2)	13.0(1)
C(52) [a]	0.581(2)	0.492(6)	0.478(2)	23.0(3)
C(53) [a]	0.488(3)	0.496(4)	0.487(2)	18.0(2)
C(54) [a]	0.469(4)	0.493(4)	0.551(2)	19.0(3)
C(55) [a]	0.436(5)	0.405(5)	0.554(3)	25.0(3)

[a] Half occupancies.

molecule of diethyl ether (i.e. 1/2 solvent molecule per cluster molecule), which was refined with fixed occupancy factors (0.5) and constrained ideal geometry. The structure was refined by full-matrix least-squares on F values, using SHELX [15]. Scattering factors were taken from ref. 16. Isotropic refinement converged to $R = 0.097$. At this stage an additional empirical absorption correction was applied [17], resulting in a further decrease of R to 0.079 (correction factors were in the range 0.78–1.27).

During the final stages of the refinement the anisotropic thermal parameters of the gold, platinum and phosphorus atoms were refined. The phenyl rings were treated as rigid groups during the refinement. The hydrogen atoms were given fixed isotropic temperature factors of 0.04 Å^2.

The final conventional agreement factors were $R = 0.063$ and $R_w = 0.078$ for the 11193 'observed' reflections and 322 variables. The function minimized was $\Sigma w(F_o - F_c)^2$ with $w = 1/(\sigma^2(F_o) + 0.0001|F_o|^2)$ with $\sigma(F_o)$ from counting statistics. The maximum shift to error ratio in the last full matrix least-squares cycle was less than 0.2. The final difference Fourier map showed residual peaks in the neighbourhood of the metal atoms of up to 1.3 e/Å^{-3}, probably due to absorption effects. At distances longer than 1.6 Å from the metal atoms the map showed no peaks higher than 0.2 e/Å^{-3}. Final positional and thermal parameters are given in Table 1, and selected bond distances and angles in Tables 2 and 3. The crystallographic number-

Table 2

Selected bond lengths (in Å) (with esd's)

Au(1)–Pt(2)	2.700(1)	Pt(3)–C(2)	2.020(13)	P(3)–C(316)	1.827(14)
Au(1)–Pt(3)	2.902(2)	Pt(3)–C(3)	2.089(14)	P(3)–C(326)	1.799(13)
Au(1)–Pt(4)	2.910(1)	Pt(4)–C(1)	2.040(11)	P(3)–C(336)	1.789(11)
Pt(2)–Pt(3)	2.702(1)	Pt(4)–C(3)	2.029(15)	P(4)–C(416)	1.855(11)
Pt(2)–Pt(4)	2.708(1)	P(1)–C(116)	1.810(9)	P(4)–C(426)	1.807(12)
Pt(3)–Pt(4)	2.666(1)	P(1)–C(126)	1.842(12)	P(4)–C(436)	1.842(10)
Au(1)–P(1)	2.285(3)	P(1)–C(136)	1.800(11)	O(1)–C(1)	1.153(13)
Pt(2)–P(21)	2.340(2)	P(21)–C(216)	1.832(8)	O(2)–C(2)	1.172(14)
Pt(2)–P(22)	2.411(3)	P(21)–C(226)	1.849(9)	O(3)–C(3)	1.173(16)
Pt(3)–P(3)	2.249(4)	P(21)–C(236)	1.846(9)	O(11)–N(1)	1.257(31)
Pt(4)–P(4)	2.260(3)	P(22)–C(246)	1.839(9)	O(12)–N(1)	1.161(33)
Pt(2)–C(1)	2.166(11)	P(22)–C(256)	1.832(9)	O(13)–N(1)	1.183(34)
Pt(2)–C(3)	2.144(14)	P(22)–C(266)	1.835(9)		

Table 3

Selected bond angles (in °) (with esd's)

Pt(2)–Au(1)–Pt(3)	57.5(1)	P(21)–Pt(2)–P(22)	109.9(1)	Pt(3)–P(3)–C(316)	117.1(4)
Pt(2)–Au(1)–Pt(4)	57.6(1)	Pt(3)–Pt(2)–C(1)	107.0(3)	Pt(3)–P(3)–C(326)	108.0(4)
Pt(3)–Au(1)–Pt(4)	54.6(1)	Pt(4)–Pt(2)–C(1)	47.9(3)	Pt(3)–P(3)–C(336)	117.2(3)
Au(1)–Pt(2)–Pt(3)	65.0(1)	Pt(3)–Pt(2)–C(2)	47.8(3)	Pt(4)–P(4)–C(416)	114.8(3)
Au(1)–Pt(2)–Pt(4)	65.1(1)	Pt(4)–Pt(2)–C(2)	106.8(3)	Pt(4)–P(4)–C(426)	115.3(4)
Au(1)–Pt(3)–Pt(2)	57.5(1)	Pt(2)–Pt(3)–C(2)	51.5(4)	Pt(4)–P(4)–C(436)	112.9(3)
Au(1)–Pt(3)–Pt(4)	62.9(1)	Pt(4)–Pt(3)–C(2)	112.0(4)	P(116)–P(1)–C(126)	105.4(5)
Au(1)–Pt(4)–Pt(2)	57.3(1)	Pt(2)–Pt(3)–C(3)	109.2(4)	C(116)–P(1)–C(136)	104.9(4)
Au(1)–Pt(4)–Pt(3)	62.5(1)	Pt(4)–Pt(3)–C(3)	48.7(4)	C(126)–P(1)–C(136)	103.7(5)
Pt(3)–Pt(2)–Pt(4)	59.0(1)	Pt(2)–Pt(4)–C(1)	52.0(3)	C(216)–P(21)–C(226)	104.5(4)
Pt(2)–Pt(3)–Pt(4)	60.6(1)	Pt(3)–Pt(4)–C(1)	112.4(3)	C(216)–P(21)–C(236)	100.6(4)
Pt(2)–Pt(4)–Pt(3)	60.4(1)	Pt(2)–Pt(4)–C(3)	110.9(4)	C(226)–P(21)–C(236)	100.0(4)
Pt(2)–Au(1)–P(1)	173.5(1)	Pt(3)–Pt(4)–C(3)	50.6(4)	C(246)–P(21)–C(256)	102.3(4)
Pt(3)–Au(1)–P(1)	128.0(1)	P(21)–Pt(2)–C(1)	100.6(3)	C(246)–P(22)–C(266)	101.9(4)
Pt(4)–Au(1)–P(1)	127.6(1)	P(21)–Pt(2)–C(2)	101.6(4)	C(256)–P(22)–C(266)	102.7(4)
Au(1)–Pt(2)–P(21)	86.1(1)	P(22)–Pt(2)–C(1)	93.0(3)	C(316)–P(3)–C(326)	106.9(5)
Au(1)–Pt(2)–P(22)	164.0(1)	P(22)–Pt(2)–C(2)	90.7(3)	C(316)–P(3)–C(336)	99.1(6)
Au(1)–Pt(3)–P(3)	132.7(1)	P(3)–Pt(3)–C(2)	101.0(4)	C(326)–P(3)–C(336)	107.5(5)
Au(1)–Pt(4)–P(4)	127.1(1)	P(3)–Pt(4)–C(3)	97.3(4)	C(416)–P(4)–C(426)	102.6(5)
Pt(3)–Pt(2)–P(21)	136.7(1)	P(4)–Pt(4)–C(1)	96.4(3)	C(416)–P(4)–C(436)	104.7(5)
Pt(4)–Pt(2)–P(21)	137.2(1)	P(4)–Pt(2)–C(3)	100.6(4)	C(426)–P(4)–C(436)	105.3(4)
Pt(3)–Pt(2)–P(22)	101.4(1)	C(1)–Pt(2)–C(2)	154.7(4)	Pt(2)–C(1)–Pt(4)	80.1(4)
Pt(4)–Pt(2)–P(22)	101.2(1)	C(2)–Pt(3)–C(3)	159.8(5)	Pt(2)–C(2)–Pt(3)	80.6(5)
Pt(2)–Pt(3)–P(3)	152.1(1)	C(1)–Pt(4)–C(3)	162.7(5)	Pt(3)–C(3)–Pt(4)	80.7(5)
Pt(4)–Pt(3)–P(3)	145.8(1)	Au(1)–P(1)–C(116)	114.1(3)	Pt(2)–C(1)–O(1)	137.2(9)
Pt(2)–Pt(4)–P(4)	148.3(1)	Au(1)–P(1)–C(126)	115.3(4)	Pt(4)–C(1)–O(1)	142.7(9)
Pt(3)–Pt(4)–P(4)	151.2(1)	Au(1)–P(1)–C(136)	112.4(4)	Pt(2)–C(2)–O(2)	139.3(10)
Au(1)–Pt(2)–C(1)	83.6(3)	Pt(2)–P(21)–C(216)	117.3(5)	Pt(3)–C(2)–O(2)	139.8(11)
Au(1)–Pt(2)–C(2)	85.9(3)	Pt(2)–P(21)–C(226)	114.6(3)	Pt(3)–C(3)–O(3)	137.0(12)
Au(1)–Pt(3)–C(2)	82.8(4)	Pt(2)–P(21)–C(236)	117.4(3)	Pt(4)–C(3)–O(3)	142.3(12)
Au(1)–Pt(3)–C(3)	90.9(4)	Pt(2)–P(21)–C(246)	115.7(3)	O(11)–N(1)–O(12)	121(4)
Au(1)–Pt(4)–C(1)	80.6(3)	Pt(2)–P(22)–C(256)	117.8(3)	O(11)–N(1)–O(13)	100(3)
Au(1)–Pt(4)–C(3)	91.8(4)	Pt(2)–P(22)–c(266)	114.3(3)	O(12)–N(1)–O(13)	124(4)

ing scheme is shown in Fig. 1, which was produced by the PLUTO program [18]. Lists of anisotropic parameters, hydrogenation coordinates, and structure factors are available from the authors.

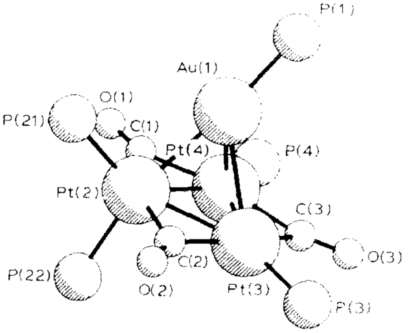

Fig. 1. Molecular configuration and atomic numbering scheme for $[Pt_3Au(\mu_2\text{-}CO)_3(PPh_3)_5]^+$.

Results and discussion

When CO was bubbled through an acetone solution of $Pt(PPh_3)_3$ and $AuPPh_3NO_3$ (I) was formed via a dark coloured intermediate. We think that $AuPPh_3^+$ strips off phosphines from $Pt(PPh_3)_3$ to form $Au(PPh_3)_2^+$ and the trinuclear $Pt_3(\mu_2\text{-}CO)_3(PPh_3)_4$, which then adds a $AuPPh_3^+$ ion to form I. This results in the overall reaction:

$$3\ Pt(PPh_3)_3 + 6\ AuPPh_3^+ + CO \rightarrow [Pt_3Au(CO)_3(PPh_3)_5]^+ + 5\ Au(PPh_3)_2^+$$

In terms of this representation, I was formed in 70% yield. In addition $[Au_6Pt(PPh_3)_7]^{2+}$ was found as a side product.

In the crystal structure determination I has C_s symmetry with the Au, Pt(2), C(3) plane as the local mirror plane (see Fig. 1). The metal frame is a distorted tetrahedron with Au on the top and a basal plane which resembles the triangular cluster $Pt_3(\mu_2\text{-}CO)_3(Pcy_3)_4$ (III). This also has C_s symmetry with three bridging CO's and P(3) and P(4) in the plane of the three Pt atoms. In I the Au atom lies at a short distance (2.700 (1) Å) to Pt(2) and at considerably greater distances to Pt(3) and Pt(4) (2.902(1) and 2.910(1) Å respectively). The angles P(1)–Au–Pt(2) and Au–Pt(2)–P(22) are 173.5(1) and 164.0(1)° respectively, so P(1), Au, Pt(2) and P(22) are roughly colinear. The Pt(2)–P(22) bond length 2.411(3) Å is longer than Pt(2)–P(21) 2.340(3) Å and Pt(3)–P(3) and Pt(4)–P(4) (2.249(4) and 2.260(3) Å, respectively). The $Pt_3(\mu_2\text{-}CO)_3$ moiety has a slight asymmetry with a Pt(3)–Pt(4) distance (2.660(1) Å) shorter than Pt(2)–Pt(3) and Pt(2)–Pt(4) (2.702(1) and 2.708(1) Å, respectively). The C atoms of the bridging CO's are closer to Pt(3) and Pt(4) (average 2.052 Å) than to Pt(2) (average 2.155 Å). A similar asymmetry was also observed in III [19]. $Pt_3(\mu_2\text{-}CO)_3(Pcy_3)_3$ is known [20], and reacts with $Au(Pcy_3)^+$ to form $Pt_3Au(\mu_2\text{-}CO)_3(Pcy_3)_4^+$ (II). This cluster has C_{3v} symmetry with equal Au–Pt bond lengths [3] (Au–Pt 2.758(5) Å).

The differences between I and II are striking. In I $AuPPh_3$ is strongly bonded to the most nucleophilic Pt site, which is evidently Pt(2), in spite of the local steric crowding. The strong Au–Pt(2) overlap is reflected in the linearity of P(1), Au, Pt(2) and P(22). The distances between Au and Pt(3) and Pt(4) are much longer, and so the interactions must be marginal. This is also reflected in the positions of P(3) and P(4), which are only slightly out of the basal plane (by 0.29 and 0.08 Å), in contrast with II where they lie well below that plane (0.71, 0.66 and 0.63 Å), so the P–Pt vectors point to the centroid of the tetrahedron, minimizing metal–metal overlap.

Like $Pt_3Au(SO_2)_2Cl(PR_3)_4$, I has 56 valence electrons in the metal cluster. Complex II, $Pt_3Au(SO_2)_3(PR_3)_4^+$ and $Pt_3Au(SO_2)(CO)_2(PR_3)_4^+$ have 54 electrons. The two extra electrons in $Pt_3Au(SO_2)_2Cl(PR_3)_4$ give rise to slightly longer Pt–Pt bond lengths than those in the 54 electron clusters, but the Pt–Au distances remain unaffected [21]. In I the two extra electrons seem to be located on Pt(2) without increase in the Pt–Pt distances, but with the marked effect on the Au–Pt bonding as described above. The ^{31}P and ^{195}Pt NMR spectra of I show interesting details, which indicate fluxionality of the phosphines. A study of the temperature and field dependencies of the NMR spectra is under way.

Acknowledgements

This work was supported in part by the Netherlands Foundation for Chemical Research (S.O.N.) and the Netherlands Technology Foundation (S.T.W.).

References

1 P.D. Boyle, B.J. Johnson, B.D. Alexander, J.A. Casalnuovo, P.R. Cannon, S.M. Johnson, E.A. Larka, A.M. Mueting and L.H. Pignolet, personal communications, to be published.

2 D.M.P. Mingos and R.W.M. Wardle, J. Chem. Soc., Dalton Trans., (1986) 73.

3 C.E. Briant, R.W.M. Wardle and D.M.P. Mingos, J. Organomet. Chem., 267 (1984) C49.

4 C.E. Briant, D.I. Gilmour and D.M.P. Mingos, J. Chem. Soc., Dalton Trans., (1986) 835.

5 P. Braunstein, H. Lehner, D.M.A. Tiripicchio, M. Tiripicchio-Camellini, Angew. Chem. Int. Ed. Engl., 23 (1984) 304.

6 W. Bos, J.J. Bour, J.J. Steggerda and L.H. Pignolet, Inorg. Chem., 24 (1985) 4298; W.P. Bosman, W. Bos, J.M.M. Smits, P.T. Beurskens, J.J. Bour and J.J. Steggerda, Inorg. Chem., 25 (1986) 2093.

7 L. Malatesta, L. Naldini, G. Simonetta and F. Cariati, Coörd. Chem. Rev., 1 (1966) 255.

8 L. William (Ed.), Inorganic-Synthesis XI, Jolly, Mc.Graw-Hill Book Company, New York, 1968, p. 105.

9 M.S. Lehman and F.K. Larsen, Acta Cryst., A30 (1974) 580.

10 D.F. Grant and E.J.J. Gabe, Appl. Cryst., 11 (1978) 114.

11 A.C.T. North, D.C. Philips and F.S. Mathews, Acta Cryst., A24 (1968) 351.

12 H. Behm and P.T. Beurskens, Z. Kristallogr., 170 (1985) 10.

13 G.M. Sheldrick, SHELX 84, Abstracts European Crystall. Meeting 8, Liege, 1983, p. 272.

14 P.T. Beurskens, W.P. Bosman, H.M. Doesburg, Th.E.M. van den Hark, P.A.J. Prick, J.H. Noordik, G. Beurskens, R.O. Gould and V. Parthasarathi, in V. Srinivasan and R.H. Sarma (Eds.), Conformation in Biology, Adenine Press, New York, 1983, p. 389.

15 G.M. Sheldrick, SHELX, A program for crystal structure determination, University Chemical Laboratory, Cambridge, England, 1976.

16 International Tables for X-ray Crystallography, Vol. IV, Birmingham, Kynoch Press, 1978.

17 N. Walker and D. Stuart, Acta Cryst., A39 (1983) 158.

18 W.O.S. Motherwell, PLUTO, a program for plotting molecular and crystal structures, University Chemical Laboratory, Cambridge, England, 1976.

19 A. Albinati, G. Garturan and A. Musco, Inorg. Chim. Acta, 16 (1976) L43.

20 A. Albinati, Inorg. Chim. Acta, 22 (1977) L31. A very great asymmetry in the bonding distances of the bridging CO's reported for this compound, has been left uncommented up till now.

21 D.I. Gilmour and D.M.P. Mingos, J. Organomet. Chem., 302 (1986) 127.